Chemosphere 315 (2023) 137743

Contents lists available at ScienceDirect

Chemosphere

journal homepage: www.elsevier.com/locate/chemosphere

Electrochemical degradation of PFOA and its common alternatives: Assessment of key parameters, roles of active species, and transformation pathway

Fatemeh Asadi Zeidabadi [a], Ehsan Banayan Esfahani [a], Sean T. McBeath [b], Kristian L. Dubrawski [c], Madjid Mohseni [a,*]

[a] Department of Chemical and Biological Engineering, University of British Columbia, 2360 East Mall, Vancouver, Canada
[b] Department of Civil and Environmental Engineering, University of Massachusetts Amherst, Amherst, MA 01002, United States
[c] Department of Civil Engineering, University of Victoria, Victoria, BC, V8P 5C2, Canada

HIGHLIGHTS

- Acidity and high temperature favor degradation, while DO has a negligible effect.
- Increasing initial concentration of PFOA has an adverse effect on the degradation.
- Electrolyte (sulfate) dosage has a dual-impact, depending on PFOA concentration.
- $SO_4^{\bullet-}$ and $^{\bullet}OH$ play key roles in PFOA degradation and defluorination, respectively.
- Degradability of PFAS in electrochemical system: 6:2 FTCA > PFOA > GenX > PFBA.

GRAPHICAL ABSTRACT

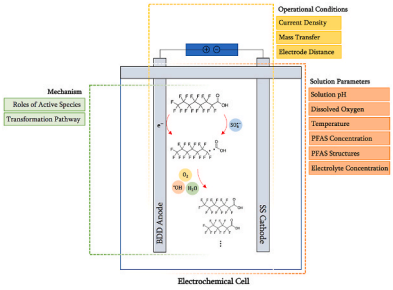

ARTICLE INFO

Handling Editor: Dr. E. Brillas

Keywords:
BDD electrooxidation
PFOA alternatives
GenX
6:2 FTCA
Fluorine recovery
Sulfate radical

ABSTRACT

This study investigates an electrochemical approach for the treatment of water polluted with per- and polyfluoroalkyl substances (PFAS), looking at the impact of different variables, contributions from generated radicals, and degradability of different structures of PFAS. Results obtained from a central composite design (CCD) showed the importance of mass transfer, related to the stirring speed, and the amount of charge passed through the electrodes, related to the current density on decomposition rate of PFOA. The CCD informed optimized operating conditions which we then used to study the impact of solution conditions. Acidic condition, high temperature, and low initial concentration of PFOA accelerated the degradation kinetic, while DO had a negligible effect. The impact of electrolyte concentration depended on the initial concentration of PFOA. At low initial PFOA dosage (0.2 mg L^{-1}), the rate constant increased considerably from 0.079 ± 0.001 to 0.259 ± 0.019 min^{-1} when sulfate increased from 0.1% to 10%, likely due to the production of $SO_4^{\bullet-}$. However, at higher initial PFOA dosage (20 mg L^{-1}), the rate constant decreased slightly from 0.019 ± 0.001 to 0.015 ± 0.000 min^{-1}, possibly due to the occupation of active anode sites by excess amount of sulfate. $SO_4^{\bullet-}$ and $^{\bullet}OH$ played important roles in decomposition and defluorination of PFOA, respectively. PFOA oxidation was initiated by one electron transfer to the anode or $SO_4^{\bullet-}$, undergoing Kolbe decarboxylation where yielded perfluoroalkyl radical followed

* Corresponding author.
E-mail address: madjid.mohseni@ubc.ca (M. Mohseni).

https://doi.org/10.1016/j.chemosphere.2023.137743
Received 7 November 2022; Received in revised form 24 December 2022; Accepted 2 January 2023
Available online 3 January 2023

three reaction pathways with $^{\bullet}OH$, O_2 and/or H_2O. PFAS electrooxidation depended on the chemical structures where the decomposition rate constants (min^{-1}) were in the order of 6:2 FTCA (0.031) > PFOA (0.019) > GenX (0.013) > PFBA (0.008). PFBA with a shorter chain length and GenX with $–CF_3$ branching had slower decomposition than PFOA. While presence of C–H bonds makes 6:2 FTCA susceptible to the attack of $^{\bullet}OH$ accelerating its decomposition kinetic. Conducting experiments in mixed solution of all studied PFAS and in natural water showed that the co-presence of PFAS and other water constituents (organic and inorganic matters) had adverse effects on PFAS decomposition efficiency.

1. Introduction

Manufacturing, applications, and disposal of fluorochemicals since the late 1940s have led to global pollution by a class of >9000 chemicals, namely per- and poly-fluoroalkyl substances (PFAS). Strict regulations concerning their adverse health impacts and the lack of installed treatment capacity in water treatment plants have triggered significant interest and efforts in developing PFAS treatment technologies. Physical-separation processes, while effective, merely transfer PFAS from one phase to another, leaving a concentrated waste stream requiring subsequent destruction technologies. Given that biodegradation of PFAS is sluggish, a variety of physico-chemical processes have been proposed for PFAS decomposition (Nzeribe et al., 2019; Trojanowicz et al., 2018). Compared to other alternatives, electrochemical processes have shown promising potential and are being adopted by industry for the abatement of PFAS, owing to their treatment efficacy and cost-effectiveness (Nzeribe et al., 2019). Electrochemical processes are carried out with the use of electrodes whose material ensures sufficiently high overpotential of oxygen evolution. Amongst the most promising materials, boron-doped diamond (BDD) electrodes have drawn increasing attention due to their fast charge-transfer kinetics, weak adsorption properties, and electrochemical stability (Chailapakul and Siangproh, 2006; McBeath et al., 2019). Applications of BDD electrodes for the degradation of PFAS have been the focus of several recent studies (Table S1) (McBeath et al., 2021). However, in spite of such efforts, there are still many open questions concerning (1) roles of active species in PFAS decomposition and their transformation pathway, (2) effects and interaction of key operational and solution parameters, and (3) degradability of different structures of PFAS in synthetic and natural waters.

Micropollutants, in general, are electrochemically degraded through direct electron transfer (DET) on the anode surface and/or by indirect oxidation via electro-generated active species. Using advanced high oxygen overpotential electrode materials like BDD, micropollutant degradation has been previously shown to be primarily mediated via hydroxyl radical ($^{\bullet}OH$) electro-generation, however other oxidants can be formed when ions (e.g., chloride, sulfate, phosphate, etc.) are present (McBeath et al., 2019). Owing to the unique structures of PFAS, the contribution of DET and the attack of active species, as well as their roles in the complex chain happening in the transformation of PFAS is not fully established and is yet the subject of further research (Radjenovic et al., 2020). In this study, sulfate was used as an electrolyte, which is a major anion in natural waters and wastewaters (Liu et al., 2019a). Electrochemical activation of sulfate electrolyte generates $SO_4^{\bullet-}$, $^{\bullet}OH$, $S_2O_8^{2-}$, and acid-base pair of $O_2^{\bullet-}/HO_2^{\bullet}$ (Liu et al., 2019a; Qian et al., 2016). Previous studies showed that $S_2O_8^{2-}$ is ineffective for the oxidation of PFOA due to the lack of unpaired electrons to attack carboxyl group (Liu et al., 2019a, 2019b). Previous reports also demonstrated that $O_2^{\bullet-}$ and $HO_2^{\bullet}$ cannot degrade PFOA (Javed et al., 2020; Qian et al., 2016). Therefore, the only potent reactive species that could contribute to the oxidation of PFOA would be $SO_4^{\bullet-}$ ($E(SO_4^{\bullet-}/SO_4^{2-}) = 2.5–3.1$ V) and $^{\bullet}OH$ ($E(^{\bullet}OH/H_2O) = 1.8–2.7$ V). There are few studies on the role of $SO_4^{\bullet-}$ and $^{\bullet}OH$ on the oxidation of PFAS using electrochemical process; however, existing literature contains contradictory results. Thus, it is important to address this question which is one of the important purposes of this paper.

The effectiveness of electrochemical degradation of PFAS is highly dependent on a number of key parameters. The majority of earlier studies considered one parameter at a time which may lead to misinterpretation of results when interactions between different parameters are present. In addition, the impacts of some parameters (e.g., PFAS initial dosage) were not investigated under conditions representative of real-world scenarios or were studied in narrow ranges, leading to contradictory results (Zhuo et al., 2012, 2020a). Studies on the influence of key parameters including dissolved oxygen (DO), temperature, mass transfer, and electrolyte concentration are either rare or still missing in the literature.

Driven by concerns regarding the impacts of legacy PFAS on the environment and humans, fluorinated chemicals with different structures, i.e., shorter chain lengths or different functional groups, have been adopted as alternatives (Wang et al., 2013). The global spread of such alternatives with even higher concentrations and similar or higher toxicity relative to legacy PFAS is evidenced in recent studies (Gomis et al., 2018; Vakili et al., 2021; Wang et al., 2019). Despite such alarming findings, little is known regarding the degradability and extent of mineralization of such emerging alternatives in electrochemical processes.

Herein, we investigated the electrochemical degradation of perfluorooctanoic acid (PFOA), a well-known PFAS, due to its extensive use and ubiquitous presence in the environment, as well as being one of the high-priority PFAS in drinking water which has been regulated in many jurisdictions worldwide (US EPA, 2022). In this study, we employed a central composite design (CCD) to investigate the effects and interactions of the main operational parameters (i.e., electrode gap, current density, and stirrer speed) on PFOA degradation. After finding the best operating condition, the effects of solution parameters such as initial pH, DO, temperature, PFOA concentration, and electrolyte concentration in broad ranges were determined. PFOA concentration and sulfate dosage were chosen to be representative of different aqueous environments (e.g., natural waters and brine solutions). Then, the roles of radicals ($^{\bullet}OH$ and $SO_4^{\bullet-}$) on the degradation and defluorination efficiencies of PFOA were clarified. This study also elucidated the transformation pathway of PFOA by analyzing the fluorine recovery, defluorination efficiency, and generation of intermediates. Lastly, the degradability and the extent of defluorination of common PFOA alternatives, i.e., its short-chain analogous (perfluorobutanoic acid (PFBA)), ether-PFAS (Hexafluoropropylene oxide dimer acid, GenX), and telomer-PFAS (6:2 fluorotelomer carboxylic acid, 6:2 FTCA), were determined. The decomposition efficiencies of all studied PFAS were also assessed in the co-presence of other PFAS and common water constituents in a natural water.

2. Methodology

2.1. Materials and experimental setup

Detailed information on chemicals and reaction setup are described in Supplementary Information (SI). Experiments were performed using a bench-scale single compartment electrochemical cell equipped with a BDD as the anode and stainless steel as the cathode. To study the kinetics of PFAS decomposition, samples were taken at specific time intervals for up to 180 min and preserved for further analysis. Experiments were

conducted in triplicate.

2.2. Experimental procedure

2.2.1. Operational and solution parameters

Effects of current density (2–10 mA cm^{-2}), electrode gap (1–2 cm), and stirring speed (400–700 rpm) on system response (PFOA degradation rate constant) were modeled by using a 3-level CCD with total runs of 18 (8 factorial, 6 axials, and 4 center points) (Table S2). After finding the best operating condition, effects of solution parameters including initial solution pH (3–9), DO (0.2–8 mg L^{-1}), temperature (10–50 °C), PFOA concentration (0.2–200 mg L^{-1}), and electrolyte concentration (0.1–10% w/v) were investigated. Full details of the CCD model and rationales for the selected operational and solution conditions are described in the SI.

2.2.2. Role of radicals/degradation pathway

A 20 mg L^{-1} PFOA solution was used for investigating the role of radicals, fluorine recovery, and degradation pathway to be able to evaluate and detect the mineralization efficiency and intermediate products. To understand the effects of $SO_4^{\bullet-}$ and $^{\bullet}OH$, degradation studies were conducted in 0.1% Na_2SO_4 (1.54 mS cm^{-1}) electrolyte and the results compared with those obtained in inert electrolytes (0.12% $NaNO_3$ and 0.17% $NaClO_4$) with the same ionic conductivities (Farhat et al., 2015; Liu et al., 2019a, 2019b). To further probe the contribution of each radical, methanol was added as a radical scavenger of both $^{\bullet}OH$ and $SO_4^{\bullet-}$ ($k_{SO4\bullet-} = 1.0 \times 10^7$ M^{-1} s^{-1}, $k_{\bullet OH} = 9.7 \times 10^8$ M^{-1} s^{-1}) to all three electrolytes (Buxton et al., 1988; Huie and Clifton, 1989). Methanol was chosen at a concentration of 70 mM which is shown to be sufficient for quenching electrogenerated radicals in the system (Fig. S2). The degradation pathway was proposed based on the intermediates detected in both negative and positive electrospray ionization modes throughout the course of experiments. Fluoride concentration was also monitored to quantify the extent of PFAS mineralization.

2.2.3. Effect of PFAS structure

The efficacy of electrochemical process for decomposition of different PFAS was investigated in deionized (DI) water and a natural water collected from Spanish Banks (SB) creek (Vancouver, Canada). 20 mg L^{-1} of PFAS was spiked in the waters such that three conditions were provided and the results were compared: i) individual PFAS in deionized water (Ind-DIW), ii) mixed PFAS in DIW (Mix-DIW), and iii) mixed PFAS in SB water (Mix-SBW). Tables S3 and S4 summarize the characteristics of the water sample and experimental conditions. 0.1% Na_2SO_4 was used as electrolyte in all solutions.

2.3. Analytical method

Concentrations of PFAS and transformation by-products were analyzed using an Agilent 1200 series uHPLC/MS system. A sample volume of 20 μL was injected onto a Waters Xterra MS C18 column proceeded by a C18 guard column. Both columns were maintained at 50 °C, and the mobile phase flow was set at 1 mL min^{-1}. The mobile phase consisted of (A) water with 20 mM ammonium acetate and (B) acetonitrile. The mobile phase concentration followed a gradient as follows (A:B): 50:50 (0 min), 10:90 (0–5 min), 50:50 (5–5.5 min), and remained at 50:50 (5.5–8 min). Solid phase extraction (SPE) was performed prior to uHPLC/MS analysis for purifying and/or concentrating samples. The concentration of fluoride ions was measured using a fluoride ion selective electrode (ISE, HI4010, Hanna Instruments). Full details of the analytical methods, limit of detection of each PFAS (Table S5) and fluoride range were reported previously (Banayan Esfahani and Mohseni, 2022) and described in the SI.

3. Results and discussion

3.1. Effect and interaction of operational parameters

The pseudo-first order rate constant of PFOA obtained with the studied operational parameters varied between 0.011 ± 0.001 and 0.079 ± 0.001 min^{-1} and are presented in Table S6. The influence of each factor and their interactions on the PFOA rate constant is displayed in the pareto chart in Fig. S4 and presented in Table S7. Based on the results, the importance of factors was in the order of stirrer speed (X3) > current density (X1) > electrode distance (X2) with regression coefficients of 0.017, 0.012, and −0.003, respectively. The regression coefficients denote the weight of factors and interactions on PFOA degradation. The data analysis showed that the linear terms of X1 and X3, the square term of X3 × X3, and interaction term of X1 × X3 were significant at the 95% confidence interval. The interaction between current density and stirrer speed (X1 × X3) had a synergistic effect, as their coefficients had a positive effect on PFOA degradation. Even if the stirrer speed (X3) had a positive impact on PFOA degradation, its square term (X3 × X3) had a negative coefficient. Main and interaction plots for PFOA rate constants were provided in Figs. S5 and S6.

3.1.1. Stirrer speed

As shown in the Pareto chart and surface plot (Fig. S7), stirrer speed had the most significant effect on PFOA degradation rate constant. Increasing the stirring speed from 400 to 700 rpm greatly enhanced the mean of PFOA rate constant from 0.030 to 0.063 min^{-1}. Increasing the stirring speed can (1) decrease the Nernst diffusion layer thickness at the electrode-solution interface and (2) increase the diffusive mass flux of PFOA to the electrode surface (Walsh, 1993) which in both cases leads to faster decomposition of PFOA. The results also showed that the degradation efficiency of PFOA increased with stirrer speed up to a point, beyond which no further increases were observed which is due to the system stabilization where further increases in mixing would have no impact on PFOA degradation.

3.1.2. Current density

With respect to PFOA degradation, current density had the second most significant effect. An increase in current density enhances PFOA degradation which is in agreement with the results of earlier studies on electrochemical oxidation of PFAS (Barisci and Suri, 2021; McBeath and Graham, 2021; Sukeesan et al., 2021). This could be due to the increase in electron transfer efficiency and the production of radical species. As shown in the main effects plot for rate constants (Fig. S5), an increase in the current density from 2 to 10 mA cm^{-2} led to an increase in the mean of PFOA rate constant from 0.040 to 0.063 min^{-1}.

3.1.3. Electrode distance

Increasing the electrode gap from 1 to 2 cm decreased the mean of PFOA rate constant from 0.057 to 0.053 min^{-1} (Fig. S5) which could be due to the longer diffusion distance (Ma et al., 2015; Zhuo et al., 2020b). However, as shown in Table S7, the electrode gap had an insignificant effect on the degradation rate constant of PFOA ($p > 0.05$) and generally was not a controlling variable during the studied range. This could be due to the fact that the electrode gap range studied in this work (1–2 cm) did not show much effect on the diffusion distance and subsequently the rate constant of PFOA.

A regression model describing the relationship between PFOA degradation rate constant (Y, min^{-1}) and the significant factors were formulated as:

$$Y = 0.057 + 0.012\ X1 + 0.017\ X3 - 0.010\ X3 \times X3 + 0.004\ X1 \times X3 \quad (1)$$

The model F-value and p-value of 38.84 and 0, respectively, infer that the model is significant (Table S8). As shown in Fig. S8, the predicted values by the model match the experimental values reasonably well with R^2 and adj-R^2 of 97.8% and 95.3%, respectively. The

regression model and experimental results revealed that the highest PFOA degradation rate constant was 0.079 ± 0.001 min^{-1}, obtained at the electrode distance of 1 cm, current density of 10 mA cm^{-2}, and stirrer speed of 700 rpm. Further experiments were performed in this condition as the best operating condition.

3.2. Effect of solution parameters

3.2.1. Initial solution pH

The effect of solution pH on PFOA degradation and defluorination was investigated at the initial pH of 3, 5.5 (without adjustment), 7, and 9. As shown in Fig. 1a acidic conditions (pH 3 and 5.5) favored the electrooxidation of PFOA. The degradation efficiencies of PFOA increased from 76.8 ± 1.8% to 96.5 ± 0.1% within 30 min as pH decreased from 9 to 3. Results observed for PFOA defluorination (Fig. 1d) showed a similar trend except for pH 3. In alkaline condition, OH^- competes with the anionic PFOA for reactive sites of the anode and suppressed the oxidation of PFOA (Zhuo et al., 2020a, 2020b). Furthermore, high solution pH converts $SO_4^{\bullet-}$ to $^{\bullet}OH$ (Eq. (2)) (Banayan Esfahani et al., 2022) whereby $SO_4^{\bullet-}$ and $^{\bullet}OH$ contribute to the decomposition and defluorination of PFOA, respectively (section 3.3). Therefore, even though the acidity is more favorable for decomposition due to the high concentration of $SO_4^{\bullet-}$, it could adversely affect the defluorination efficiency given the less amount of $^{\bullet}OH$ in the solution.

$$SO_4^{\bullet-} + OH^- \rightarrow SO_4^{2-} + {}^{\bullet}OH, \quad k = 8.3 \times 10^7 M^{-1} s^{-1} \tag{2}$$

3.2.2. Initial dissolved oxygen (DO)

As depicted in Fig. 1b and e, results obtained in open-air (DO = 8 mg L^{-1}) and oxygen-free (DO = 0.2 mg L^{-1}) environments showed the negligible role of DO on degradation and defluorination of PFOA ($p > 0.05$). In both environments, DO reached the same concentration (~6 mg L^{-1}) roughly 10 min after the start of the experiments (Fig. S9). In open-air system, the DO concentration decreased from 8 to ~6 mg L^{-1} due to the possible involvement of O_2 in the decomposition mechanism of PFOA (section 3.4.2). Whereas, in the oxygen-free environment, DO increased and reached the same value (~6 mg L^{-1}), given the evolution of O_2 in the system (Eq. S4). Therefore, we would not expect to see significant differences in PFOA decomposition in the two systems after the DO got stabilized (>10 min). However, we still did not see any difference in the first 10 min, implying that DO is not an important parameter to control in practical purposes.

3.2.3. Solution temperature

As shown in Fig. 1c and f, elevating the temperature from 10 to 22 °C significantly increased PFOA degradation (83.3–90.7%) and defluorination (60.4–68.2%) efficiencies. However, further increase of the temperature in the wide range of 22–50 °C only slightly affected the oxidation, increasing the degradation and defluorination efficiencies from 90.7 to 94.6% and 68.2–70.3%, respectively. Applying Arrhenius equation (Eq. S3), the apparent activation energy (E_{app}) of PFOA was determined to be 8.3 ± 1.7 kJ mol^{-1} (Fig. S10), implying a slight positive effect of temperature on PFOA degradation (Brahim et al., 2016). This observation could be attributed to the lower viscosity of water at higher temperatures which leads to a higher conductivity and mass transfer efficiency. Also, the elevated temperature is likely to activate the electrode surface and maintain more active sites on the electrode (Asghari and Yoshida, 2008).

3.2.4. Initial PFOA concentration

As shown in Fig. 2, increasing the initial concentration of PFOA from 0.02 to 20 mg L^{-1} decreased the decomposition efficiency from 100 to 68.9 ± 0.7%. However, at the higher dosage of 20–200 mg L^{-1}, the

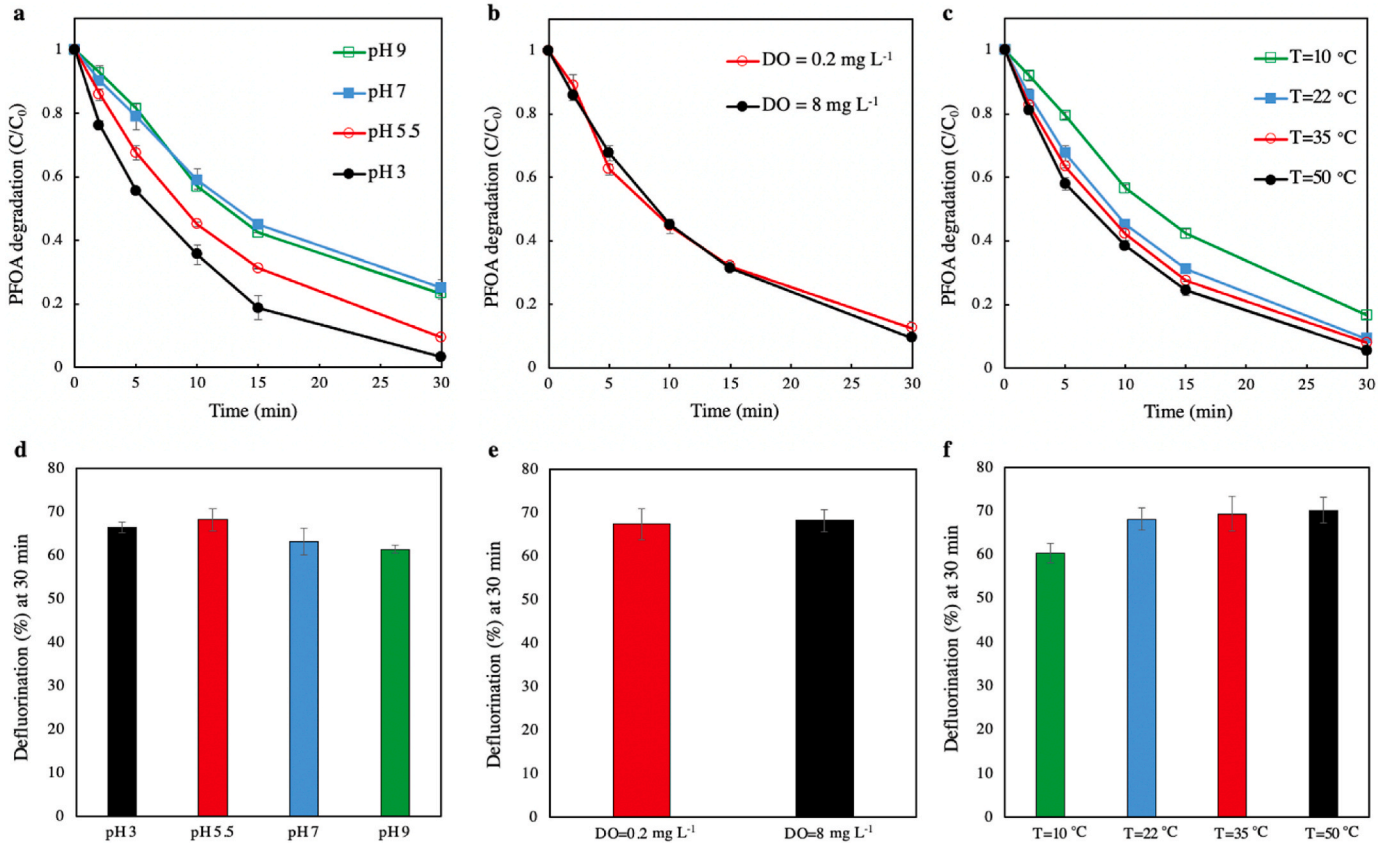

Fig. 1. Effect of a and d) solution pH, b and e) DO, and c and f) temperature on PFOA degradation (C/C_0) and defluorination (%). Experimental conditions: CD = 10 mA cm^{-2}, d = 1 cm, n = 700 rpm, $[PFOA]_0$ = 0.2 mg L^{-1}, $[Na_2SO_4]$ = 0.1% w/v.

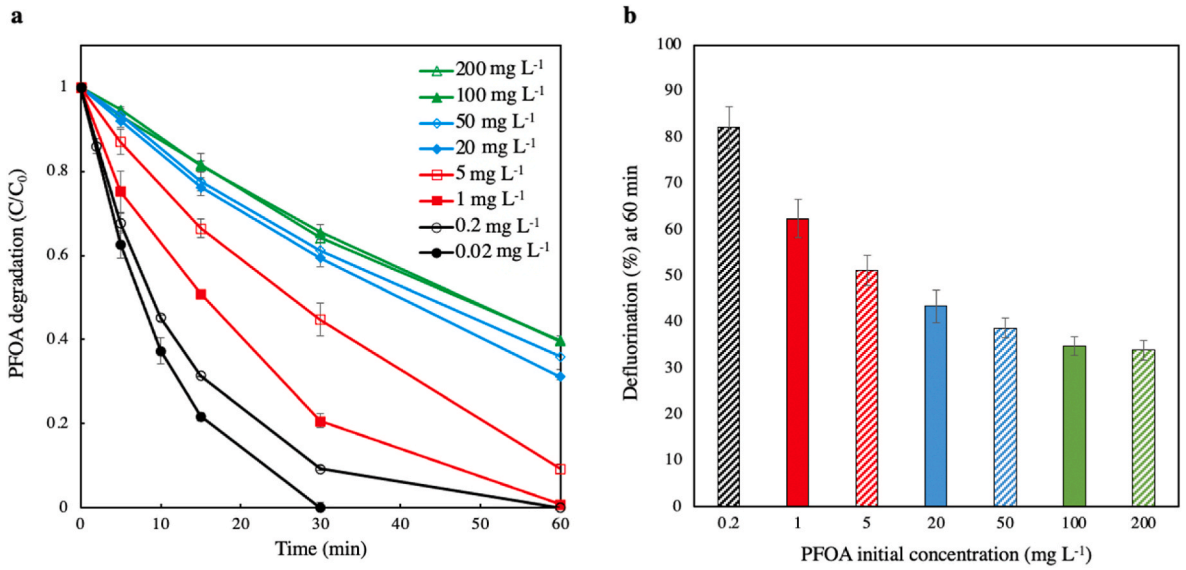

Fig. 2. Effect of PFOA initial concentration on its degradation (C/C_0) and defluorination (%). Experimental conditions: CD = 10 mA cm^{-2}, d = 1 cm, n = 700 rpm, $[Na_2SO_4]$ = 0.1% w/v.

initial concentration of PFOA had a trivial effect on both degradation and defluorination efficiencies. Increasing PFAS concentration can have contrasting effects. On the one hand, it could prohibit the degradation efficacy by increasing the concentration of short-chain intermediates which would competitively consume electrogenerated reactive radicals (e.g., $SO_4^{\bullet-}$) formed in the solution. Moreover, these intermediates would also compete for the reactive sites on the anode surface, thereby decreasing the degradation of PFOA as well as the electro-generation of reactive radicals (e.g., $SO_4^{\bullet-}$), leading to a lower current efficiency towards PFOA degradation (Barisci and Suri, 2021). On the other hand, increasing the initial PFOA concentration can enhance the diffusive mass flux of PFOA to the anode surface due to an increase in concentration gradient across the Nernst diffusion layer, as described by Fick's Law of diffusion (Zhuo et al., 2020a, 2020b). Therefore, in lower concentrations, the adverse effect of generated intermediates outweighed the promotive effect of increased mass transfer towards the electrode surface. However, at the higher dosage, the initial concentration of PFOA had a negligible effect on the degradation rate constant, demonstrating a balance between aforementioned contrasting effects.

3.2.5. *Electrolyte concentration*

The effect of electrolyte concentration on PFOA degradation was investigated in two conditions with low (0.2 mg L^{-1}) and high (20 mg L^{-1}) concentrations of PFOA. As illustrated in Fig. 3, in low PFOA concentration, the PFOA reaction rate increased considerably from 0.079 ± 0.001 to 0.259 ± 0.019 min^{-1} by increasing the initial concentration of sulfate from 0.1% to 10%. In contrast, in high PFOA concentration, the reaction rate slightly decreased from 0.019 ± 0.001 to 0.015 ± 0.000 min^{-1} in 0.1%–10% sulfate concentration. In the presence of Na_2SO_4, strong oxidizing $SO_4^{\bullet-}$ can be electro-generated through DET to the anode or reaction with $^{\bullet}OH$, whereby the latter predominates in acidic conditions (pH < 2) where HSO_4^- and H_2SO_4 are present (Liu et al., 2019b). Due to the pH conditions that were measured in the bulk water solution throughout electrolysis (pH > 3, see Fig. S11), it is

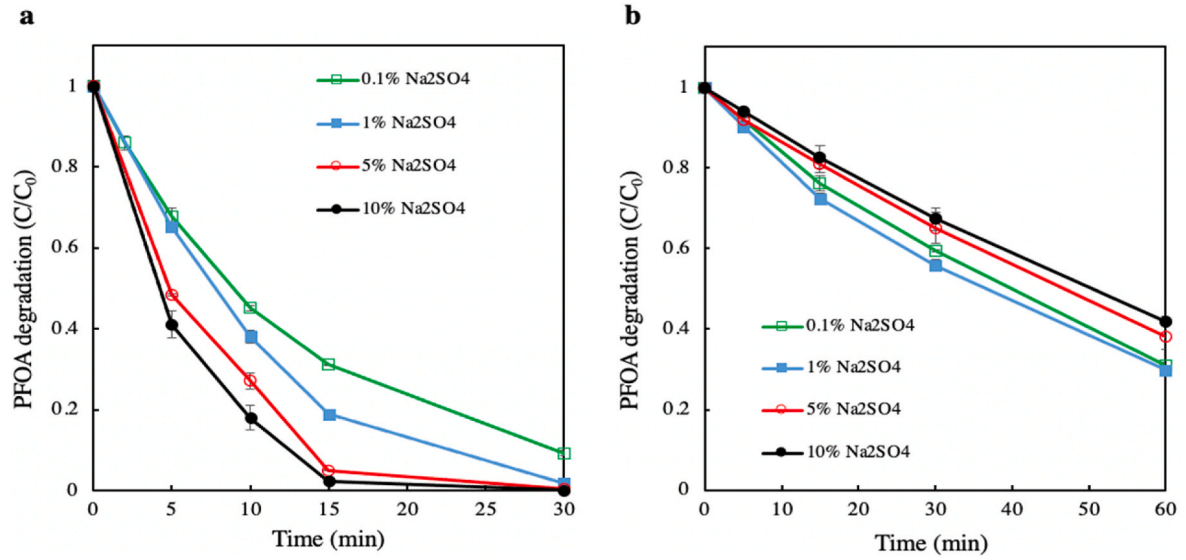

Fig. 3. Effect of electrolyte concentration on PFOA degradation (C/C_0) a) [PFOA] = 0.2 mg L^{-1} b) [PFOA] = 20 mg L^{-1}. Experimental conditions: CD = 10 mA cm^{-2}, d = 1 cm, n = 700 rpm.

believed that DET at the anode surface is the main pathway for $SO_4^{\bullet-}$ formation. Given these results, an increasing sulfate concentration can have two contrasting effects: facilitating PFOA decomposition by electro-generated $SO_4^{\bullet-}$ or suppressing the degradation efficacy by competing with PFOA for the reactive sites of the anode. In low initial PFOA condition, where the reaction is mostly mass transfer limited, the promotive effect of $SO_4^{\bullet-}$ is dominant since the reaction is not limited by the reactive sites that are occupied by the sulfate ions being oxidized on the surface. However, in high initial concentration of PFOA, where the reaction is mostly kinetically limited, the availability of active sites is an important factor which governs the reaction kinetics. Therefore, the inhibitory effect (i.e., competing for the anode active sites) of sulfate concentration overcame its promotive effect, decreasing the degradation rate of PFOA. Results presented herein demonstrate that BDD electro-oxidation is effective for the treatment of PFAS in aqueous environments containing sulfate and could also be implemented to degrade PFAS in solutions containing high concentration of salt, allowing to combine removal and degradation processes. In this combination, waste stream of separation/removal process containing high concentrations of PFAS and salts (commonly 10% (Dixit et al., 2020),) can be treated efficiently by electrochemical process.

Table S1 presents a comparison with previous studies on PFAS (mainly PFOA) decomposition using electrochemical processes by BDD anode. In the present study, PFOA electrooxidation has been carried out in a wide range of operational and solution parameters, which make the comparison with other studies more feasible given that earlier studies were conducted in a broad range of parameters (e.g., PFOA concentration ranges 0.3–100 mg L^{-1}, Table S1). In the present study, 69.0% and 43.4% degradation and defluorination of 20 mg L^{-1} PFOA were obtained within 60 min, which were in agreement with the results reported in previous studies (Uwayezu et al., 2021; Yang et al., 2019). However, Uwayezu performed experiments in two-fold greater current density (21.4 mA cm^{-2}), using BDD as both cathode and anode, which is an important consideration in practical applications. Compared with studies that worked at low concentration of PFAS, the PFOA decomposition rate constant reported by Schaefer et al. (2017) was one order of magnitude lower than that obtained in this study (0.2 mg L^{-1} initial PFOA). However, Schaefer et al. used a higher current density and a Tungsten cathode, which adds a significant increase in the material cost associated with the process.

3.3. Role of radicals ($^{\bullet}OH$ and $SO_4^{\bullet-}$)

According to Fig. 4a, the decomposition kinetic of PFOA in sulfate electrolyte (0.019 ± 0.001 min^{-1}) was faster than those obtained in nitrate (0.014 ± 0.00 min^{-1}) and perchlorate (0.013 ± 0.001 min^{-1}) as inert electrolytes. Since $^{\bullet}OH$ is produced in all three electrolyte solutions, the enhanced rate constant was very likely due to the indirect oxidation of PFOA by $SO_4^{\bullet-}$. Moreover, the addition of methanol to perchlorate and nitrate electrolytes did not affect the degradation efficiencies, while the efficacy declined from 68.9 ± 0.7% to 54.8 ± 0.3% in sulfate electrolyte within 60 min. This further confirms the role of $SO_4^{\bullet-}$ owing to the scavenging effect of methanol for both $^{\bullet}OH$ and $SO_4^{\bullet-}$. Even though the presence of $SO_4^{\bullet-}$ enhanced the degradation efficiency by ~14%, the ~55% decomposition was due to the DET, implying that PFOA decomposition is predominantly governed by DET to the anode surface. On the other hand, the defluorination efficacies of all three electrolytes were almost the same, 44.8 ± 0.9, 44.1 ± 1.9, and 42.7 ± 0.4% within 60 min and decreased to 37.2 ± 0.9, 36.3 ± 2.9, and 33.8 ± 2.4% in the presence of methanol using sulfate, nitrate, and perchlorate electrolytes, respectively (Fig. 4b). In other words, the addition of methanol decreased the defluorination efficiencies to a similar extent in the presence of all three electrolytes. This observation confirmed the role of $^{\bullet}OH$ in defluorination of PFOA (section 3.4.2), even though it has a negligible effect on the initial oxidation.

3.4. By-product formation and decomposition pathway

3.4.1. By-product formation and fluorine recovery

Incomplete defluorination and the gap between degradation and defluorination efficiencies (Fig. S12) suggested the formation of F-containing intermediates during PFOA degradation. To extend our understanding of the generated intermediates, we considered different pathways and the products that could be generated in those ways. The first possible category of intermediates was the formation of organosulfates ($R–OSO_3^-$) and hydroxysulfates ($HO\text{-}R\text{-}OSO_3^-$) in the presence of $SO_4^{\bullet-}$ which was proposed by Van Buren et al. (2021). We screened 4 compounds with m/z ratios of 465 ($C_7F_{15}–OSO_3^-$), 415 ($C_6F_{13}–OSO_3^-$), 482 ($HO–C_7F_{15}–OSO_3^-$), and 432 ($HO–C_6F_{13}–OSO_3^-$) but did not detect any of the intermediates. The second attempt was detection of $C_nF_{2n+1}OH/H$. We screened m/z ratios of 386 ($C_7F_{15}OH$), 370 ($C_7F_{15}H$), 336 ($C_6F_{13}OH$), and 320 ($C_6F_{13}H$) in both negative and positive modes and were not able to detect any of these intermediates, even in very high concentrations of PFOA up to 500 mg L^{-1}, which could be due to the

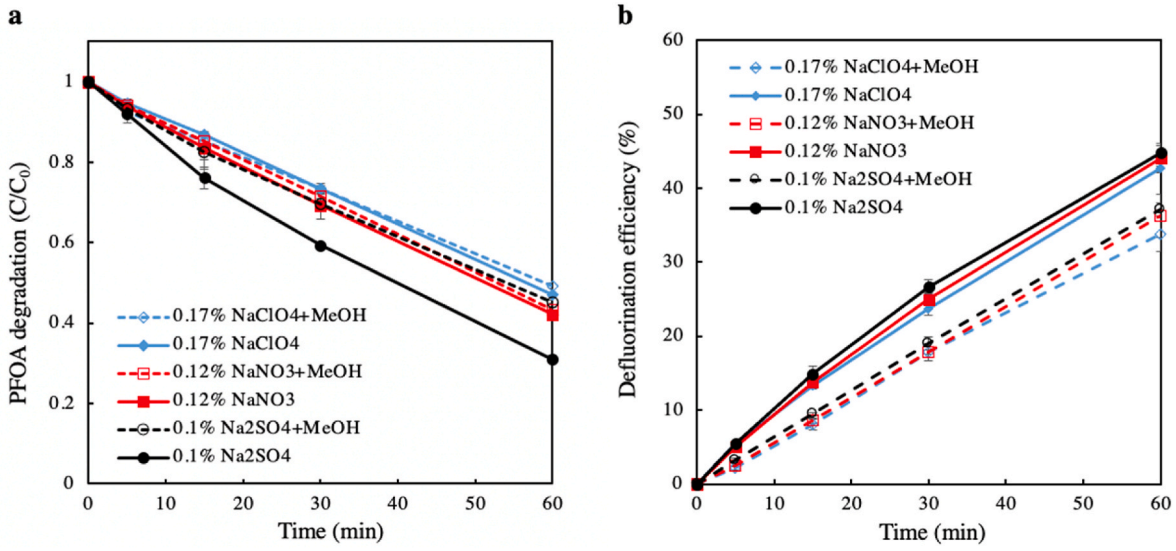

Fig. 4. PFOA degradation (C/C_0) (a) and defluorination efficacy (%) (b) in Na_2SO_4, $NaNO_3$, and $NaClO_4$ electrolytes in the presence and absence of methanol.

instability of these by-products (Babu et al., 2022; Olvera-Vargas et al., 2022). Shorter chain perfluorocarboxylic acids (PFCAs, $C_nF_{2n+1}COO^-$) were the third category with n from 2 to 6 that were detected and quantified. CF_3COO^- or TFA was analyzed but not detected even in very high concentrations of parent PFOA up to 500 mg L^{-1} which could be due to its transformation into the gas phase (as the main reason since TFA is volatile) and/or adsorption to the surface of BDD anode (Carter and Farrell, 2008; Nzeribe et al., 2019; Uwayezu et al., 2021). Fig. 5a shows the concentration of these intermediates versus time. As indicated, concentrations of the generated by-products were time-dependent where they first increased, reached a peak, and then decreased, indicating their formation and subsequent degradation. The maximum concentrations of PFHpA ($C_6F_{13}COO^-$), PFHxA ($C_5F_{11}COO^-$), PFPeA ($C_4F_9COO^-$), PFBA ($C_3F_7COO^-$), and PFPrA ($C_2F_5COO^-$) were obtained at 30, 60, 90, 90, and 120 min, respectively, implying a stepwise decomposition of PFOA. Moreover, longer chain intermediates were degraded faster compared to the shorter chains due to the effect of chain length on the degradation efficacy of PFCAs (Fig. S13).

Fluorine recovery of PFOA, presenting the molar ratio of the total fluorine in the form of PFOA, its generated by-products, and fluoride versus time was established and shown in Fig. 5c. Concentration of shorter chain intermediates was very low compared to that of PFOA (<1%), indicating their simultaneous formation and degradation. The total recovery of fluorine in this process decreased to 80.7% within 60 min of electrolysis and was subsequently kept relatively constant. The decreases in fluorine recovery were attributed to 3 main phenomena: (1) possible formation of volatile fluorinated by-products such as F_2, CHF_3, CF_4, C_2F_6, and TFA (Ochiai et al., 2011; Radjenovic et al., 2020; Uwayezu et al., 2021), (2) formation of intermediates from other reaction pathways that were not identified, and (3) little release of the reaction intermediates to the bulk water solution, given that the decomposition of PFOA mainly occurs on the electrode surface. However, with such high recoveries of fluorine, it is plausible to derive the main reaction mechanism of electrochemical mineralization of PFOA according to the detected intermediates.

Comparing the results of by-product formation and fluorine recovery at 0.1 and 10% electrolyte (Na_2SO_4) concentration revealed a slightly different behaviour between the two conditions (Fig. 5b and d). Similar to the earlier observation for PFOA, generated C4–C6 PFCAs with low concentrations of ~0.2 mg L^{-1} degraded faster in 10% sulfate electrolyte where nearly complete degradation was reached within 120 and 180 min in 10 and 0.1% sulfate concentrations, respectively. To further confirm these results, the degradation efficacy of PFHpA (C6) was compared in the two sulfate concentrations (Fig. S14), which agreed with the data presented above. In addition, fluorine recovery of PFOA at 10% sulfate was lower than that of 0.1%. Given the low concentration of fluorine in the form of intermediates compared to that in the form of fluoride and PFOA, the main reason for this difference could be attributed to the defluorination efficiencies obtained in 0.1% and 10% sulfate, 76.7% and 62.3% at 180 min, respectively. The high defluorination efficacy in low electrolyte concentrations might be due to the lower conductivity of solution resulting in a higher voltage which is a driving force for breaking the C–F bonds (Urtiaga et al., 2015; Uwayezu et al., 2021).

3.4.2. Decomposition pathway

Considering the results obtained in this study and literature review, a possible degradation pathway was proposed for PFOA, as demonstrated in Fig. 6. It is generally accepted that direct defluorination of PFCAs through nucleophilic substitution is almost impossible due to the strong

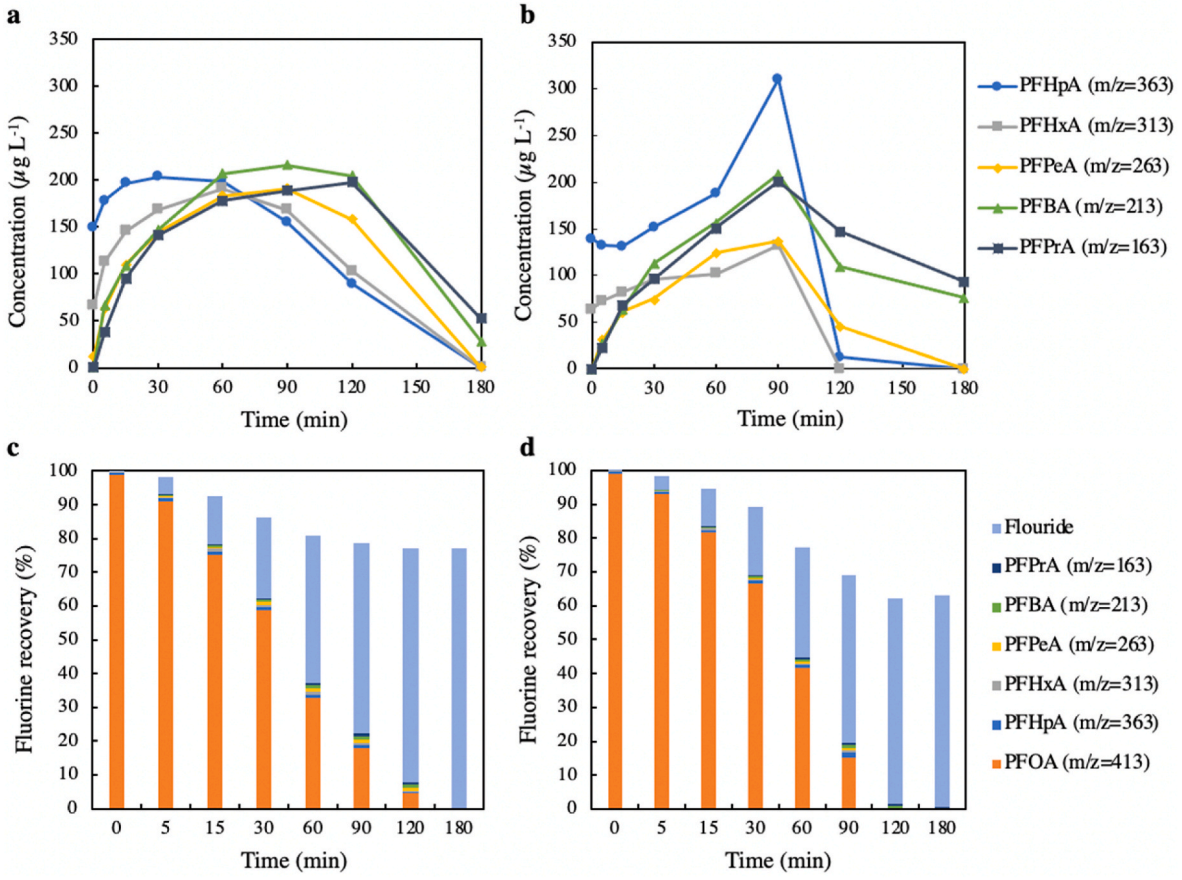

Fig. 5. Evolution of intermediates (a, [Na_2SO_4] = 0.1% w/v - b, [Na_2SO_4] = 10% w/v) and fluorine recovery (c, [Na_2SO_4] = 0.1% w/v - d, [Na_2SO_4] = 10% w/v) during PFOA decomposition. Experimental conditions: [PFOA] = 20 mg L^{-1}, CD = 10 mA cm^{-2}, d = 1 cm, n = 700 rpm.

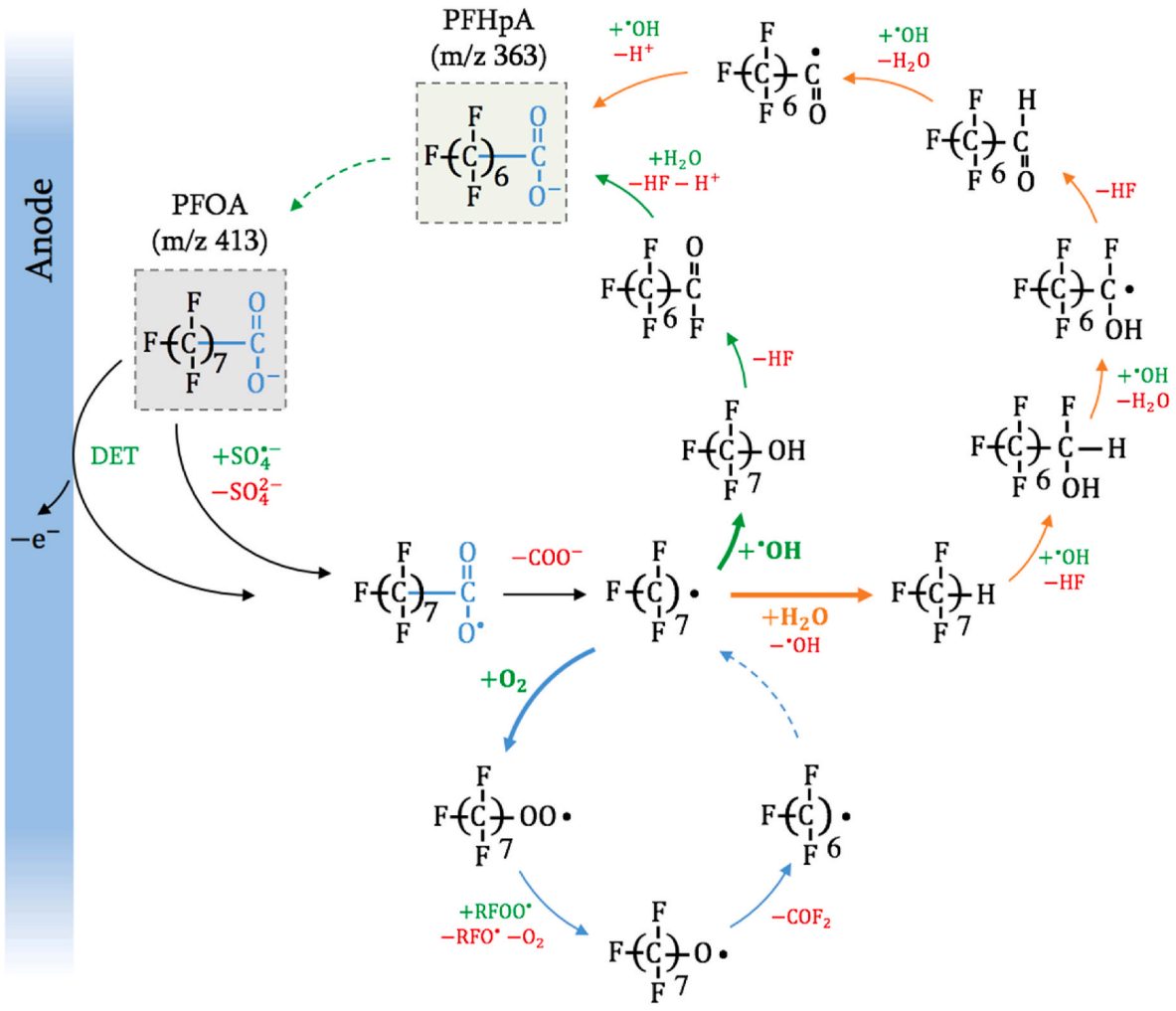

Fig. 6. Decomposition mechanism of PFOA through DET or oxidation by sulfate radical.

C–F bond (Lin et al., 2013). Experimental results also showed the negligible reactivity of •OH with PFOA, given that •OH typically reacts via an H atom abstraction with the saturated organics. Considering the contribution of $SO_4^{\bullet-}$ on the initial transformation of PFOA, the oxidation is initiated by an electron transfer from carboxyl head group to the anode surface and/or $SO_4^{\bullet-}$ to form highly reactive PFCA radical ($C_7F_{15}COO^{\bullet}$). This radical undergoes Kolbe decarboxylation and yields perfluoroalkyl radical ($C_7F_{15}^{\bullet}$). The produced $C_7F_{15}^{\bullet}$ then follows three reaction pathways. One way is the reaction of $C_7F_{15}^{\bullet}$ with •OH. Unlike the negligible role of •OH in the initial degradation of PFOA, its role in defluorination is significant, as discussed in section 3.3. This reaction yields an unstable alcohol $C_7F_{15}OH$ which undergoes hydrolysis and HF release yielding shorter chain PFCA ($C_6F_{13}COO^-$). In the second pathway, $C_7F_{15}^{\bullet}$ undergoes hydrolysis to form $C_7F_{15}H$ which with further reactions with •OH and release of HF generates $C_6F_{13}COO^-$. The generated $C_6F_{13}COO^-$ is further decomposed to shorter chain PFCAs in a similar pathway. Thirdly, the generated $C_7F_{15}^{\bullet}$ may react with oxygen produced from water electrolysis to form perfluoroalkyl peroxy radical ($C_7F_{15}OO^{\bullet}$) (Zhuo et al., 2016). As shown in Fig. S9, upon the start of the experiment, solution DO dropped from 8 mg L^{-1} to 6 mg L^{-1}, indicating the possible involvement of oxygen in PFAS mineralization pathway. Two perfluoroalkyl peroxy radicals combine to form $C_7F_{15}O^{\bullet}$. Since the generated molecule is unstable, it is decomposed to shorter perfluoroalkyl radical ($C_6F_{13}^{\bullet}$) and COF_2.

3.5. Degradability of different structures of PFAS

As indicated in Fig. 7a, the degradation rate constants were observed to be increased in the order of 0.008 ± 0.000, 0.013 ± 0.000, 0.019 ± 0.001, and 0.031 ± 0.002 min^{-1} for PFBA, GenX, PFOA, and 6:2 FTCA, respectively. In general, the shorter the chain length increases the solubility of PFAS in water which hinders their adsorption on the anode surface, in turn, reduces the rate constant (Zhuo et al., 2012). The results also indicated the lower degradation rate of GenX compared to PFOA which could be due to the presence of $–CF_3$ branch at the α-position hindering effective electron transfer from the carboxylic head group (Babu et al., 2022). Moreover, 6:2 FTCA showed the fastest rate constant among all the studied PFAS which could be attributed to the attack of •OH to the unsaturated C–H bond (Carrillo-Abad et al., 2018). Furthermore, different degradability of PFAS could be a consequence of the effect of molecular polarizability (α_p) predicted by Radjenovic et al. (2020) using the density functional theory (DFT) modeling. Molecular polarizability is defined as the ability of a molecule to form a dipole in an electric field and thus is a descriptor of the rate of electron transfer. α_p (C m^2 V^{-1}) decreases in the order of PFOA (140), GenX (114) and PFBA (77.5), which is consistent with the trend observed in Fig. 7a (Duinslaeger and Radjenovic, 2022; Radjenovic et al., 2020). Fig. 7b also presents the defluorination efficiency of four studied PFAS. At the beginning of the electrolysis, the defluorination followed the same trend as the degradation, however, after a while the defluorination efficiencies of GenX and PFBA surpassed those of PFOA and 6:2 FTCA. Fewer number of intermediates in PFBA and GenX may be the main reason for

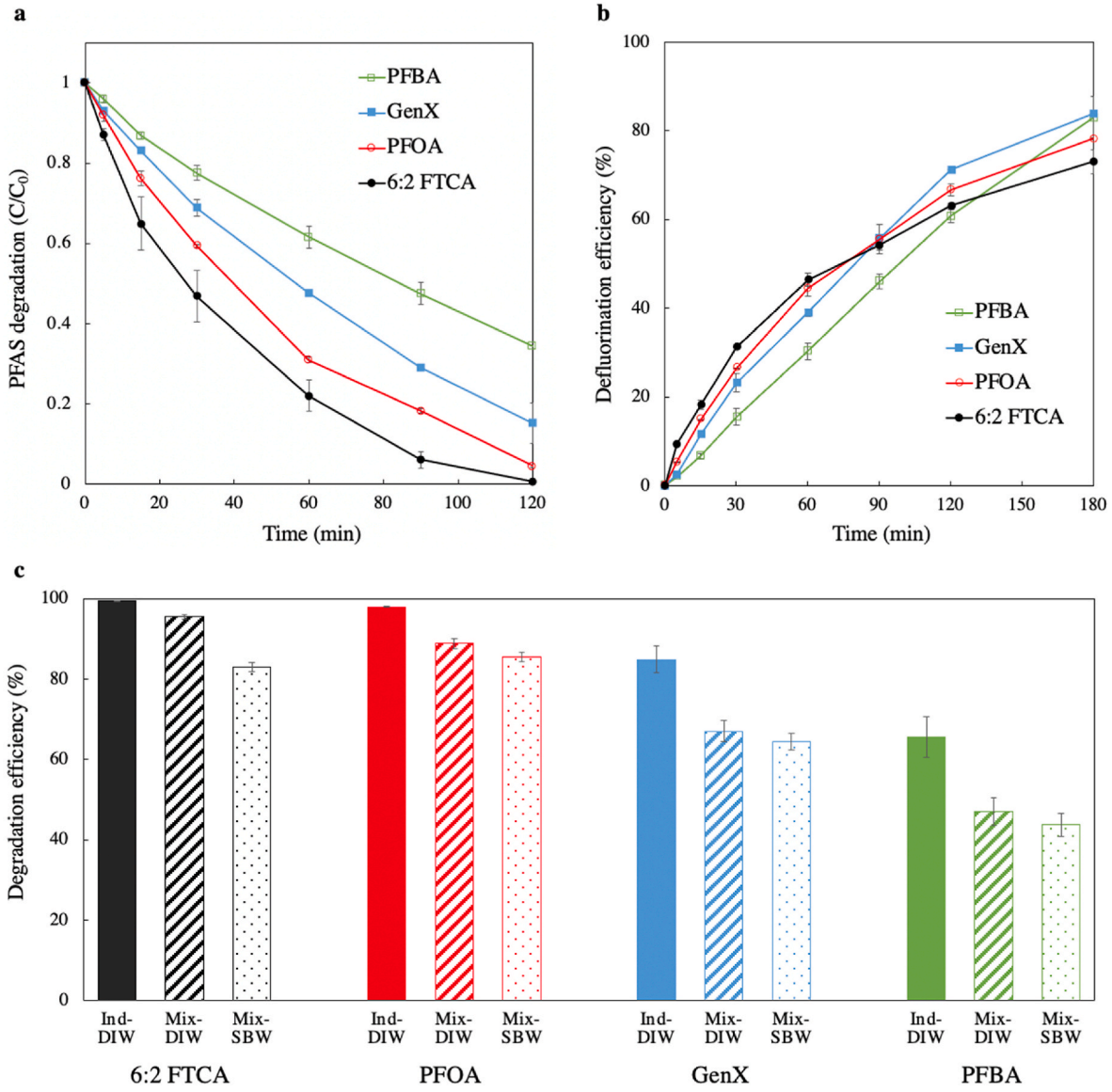

Fig. 7. Effect of PFAS structure on a) degradation (C/C_0) and b) defluorination efficiency (%). c) Effects of PFAS mixture and water matrix on PFAS degradation within 120 min. Experimental conditions: [PFAS] = 20 mg L^{-1}, [Na_2SO_4] = 0.1% w/v, CD = 10 mA cm^{-2}, d = 1 cm, n = 700 rpm.

higher defluorination efficacies of these PFAS. The role of radicals and decomposition pathways of PFOA alternatives are currently under examination in our lab. The results indicated BDD electro-oxidation as a promising approach that can be implemented in the existing fluorochemical production plants that release various PFAS into the water stream.

Fig. 7c shows the degradation efficiencies of studied PFAS in three different matrices including Ind-DIW, Mix-DIW, and Mix-SBW. When performing in a mixed solution containing all PFAS, lower decomposition efficiencies were observed for all PFAS compared to the ones in individual solutions. It could be mainly due to the competition between PFAS for occupying the active sites of the BDD anode. The observed decrease is more salient in the case of GenX and PFBA due to the faster decomposition kinetics of 6:2 FTCA and PFOA which outcompeted GenX and PFBA degradation. However, comparing the results of Mix-DIW and Mix-SBW showed a slight decrease in PFOA, PFBA, and GenX decomposition which could be due to the low concentrations of organic and inorganic matters presented in the SBW indicating the high efficacy of electrochemical system for treatment of natural water bodies. However, for the case of 6:2 FTCA, 95.5% and 83.0% degradation efficiencies were observed in Mix-DIW and Mix-SBW, respectively, which could be attributed to the presence of $^{\bullet}OH$ scavengers (e.g., bicarbonate and DOC) in SBW.

4. Conclusions

The electrochemical decomposition of PFOA on a BDD electrode in the presence of sulfate electrolyte was examined. The highest PFOA decomposition rate was achieved by combining a high current density and stirrer speed, the two main operating parameters. Acidic condition, high temperature, and low initial concentration of PFOA accelerated the degradation kinetic, while DO had a negligible effect on the decomposition of PFOA. Electrolyte concentration had a dual-impact; generation of $SO_4^{\bullet-}$ could promote degradation, while occupying the active sites by sulfate ions could prohibit the degradation depending on the initial concentration of PFOA. $SO_4^{\bullet-}$ and $^{\bullet}OH$ played important roles in decomposition and defluorination of PFOA, respectively. PFOA oxidation was initiated by one electron transfer to the anode or $SO_4^{\bullet-}$, undergoing Kolbe decarboxylation where yielded perfluoroalkyl radical followed three reaction pathways with $^{\bullet}OH$, O_2, and/or H_2O forming

shorter chain PFCAs as the main intermediates. PFAS electrooxidation depends on the chain length and structure, where shorter chain length species PFBA and $-CF_3$ branching species GenX had slower decomposition when compared to PFOA, while the presence of C–H bonds in 6:2 FTCA made it susceptible to $^{\bullet}OH$ attack, accelerating its decomposition kinetic. Conducting experiments in mixed solution of all studied PFAS and in natural water showed that the co-presence of PFAS and other water constituents (organic and inorganic matters) had adverse effect on PFAS decomposition efficiency.

Credit author statement

Fatemeh Asadi Zeidabadi: Experimental work; Data collection and analysis; Manuscript draft writing and preparation. **Ehsan Banayan Esfahani:** Data analysis; Manuscript draft writing and review. **Sean T. McBeath:** Advice on experimental work; Data review; Reviewing and editing the manuscript. **Kristian Dubrawski:** Advice, Reviewing and editing the manuscript. **Madjid Mohseni**: Funding; Supervision; Reviewing and editing the manuscript.

Declaration of competing interest

The authors declare that they have no known competing financial interests or personal relationships that could have appeared to influence the work reported in this paper.

Data availability

Data will be made available on request.

Acknowledgement

The financial support from the Natural Sciences and Engineering Research Council of Canada (NSERC) is greatly appreciated. The authors would like to acknowledge Benjamin Herring from the UBC Chemistry Department for assisting with the PFAS analysis. We also thank William Chen for providing Spanish Bank Creek water for the experiments.

Appendix A. Supplementary data

Supplementary data to this article can be found online at https://doi.org/10.1016/j.chemosphere.2023.137743.

References

Asghari, F.S., Yoshida, H., 2008. Electrodecomposition in subcritical water using o-xylene as a model for benzene, toluene, ethylbenzene, and xylene pollutants. J. Phys. Chem. A 112, 7402–7410. https://doi.org/10.1021/jp800452s.

Babu, S.D., Mol, J.M.C., Buijnsters, J.G., 2022. Experimental insights into anodic oxidation of hexafluoropropylene oxide dimer acid (GenX) on boron-doped diamond anodes. Chemosphere 288, 132417. https://doi.org/10.1016/j.chemosphere.2021.132417.

Banayan Esfahani, E., Asadi Zeidabadi, F., Zhang, S., Mohseni, M., 2022. Photochemical/catalytic oxidative/reductive decomposition of per- and poly-fluoroalkyl substances (PFAS), decomposition mechanisms and effects of key factors: a review. Environ. Sci. Water Res. Technol. 8, 698–728. https://doi.org/10.1039/D1EW00774B.

Banayan Esfahani, E., Mohseni, M., 2022. Fluence-based photo-reductive decomposition of PFAS using vacuum UV (VUV) irradiation: effects of key parameters and decomposition mechanism. J. Environ. Chem. Eng. 10, 107050 https://doi.org/10.1016/j.jece.2021.107050.

Barisci, S., Suri, R., 2021. Electrooxidation of short- and long-chain perfluoroalkyl substances (PFASs) under different process conditions. J. Environ. Chem. Eng. 9 https://doi.org/10.1016/j.jece.2021.105323.

Brahim, M. Ben, Belhadj Ammar, H., Abdelhédi, R., Samet, Y., 2016. Electrochemical removal of the insecticide imidacloprid from water on a boron-doped diamond and Ta/PbO 2 anodes using anodic oxidation process. Kor. J. Chem. Eng. 33, 2602–2609. https://doi.org/10.1007/s11814-016-0128-0.

Buxton, G.V., Greenstock, C.L., Helman, W.P., Ross, A.B., 1988. Critical Review of rate constants for reactions of hydrated electrons, hydrogen atoms and hydroxyl radicals (·OH/·O− in Aqueous Solution. J. Phys. Chem. Ref. Data 17, 513–886. https://doi.org/10.1063/1.555805.

Carrillo-Abad, J., Pérez-Herranz, V., Urtiaga, A., 2018. Electrochemical oxidation of 6:2 fluorotelomer sulfonic acid (6:2 FTSA) on BDD: electrode characterization and mechanistic investigation. J. Appl. Electrochem. 48, 589–596. https://doi.org/10.1007/s10800-018-1180-8.

Carter, K.E., Farrell, J., 2008. Oxidative destruction of perfluorooctane sulfonate using boron-doped diamond film electrodes. Environ. Sci. Technol. 42, 6111–6115. https://doi.org/10.1021/es703273s.

Chailapakul, O., Siangproh, W., 2006. Boron-doped diamond-based sensors: a review. Sens. Lett. 4, 99–119. https://doi.org/10.1166/sl.2006.008.

Dixit, F., Barbeau, B., Mostafavi, S.G., Mohseni, M., 2020. Removal of legacy PFAS and other fluorotelomers: optimized regeneration strategies in DOM-rich waters. Water Res. 183, 116098 https://doi.org/10.1016/j.watres.2020.116098.

Duinslaeger, N., Radjenovic, J., 2022. Electrochemical degradation of per- and polyfluoroalkyl substances (PFAS) using low-cost graphene sponge electrodes. Water Res. 213, 118148 https://doi.org/10.1016/j.watres.2022.118148.

Farhat, A., Keller, J., Tait, S., Radjenovic, J., 2015. Removal of persistent organic contaminants by electrochemically activated sulfate. Environ. Sci. Technol. 49, 14326–14333. https://doi.org/10.1021/acs.est.5b02705.

Gomis, M.I., Vestergren, R., Borg, D., Cousins, I.T., 2018. Comparing the toxic potency in vivo of long-chain perfluoroalkyl acids and fluorinated alternatives. Environ. Int. 113, 1–9. https://doi.org/10.1016/j.envint.2018.01.011.

Huie, R.E., Clifton, C.L., 1989. Rate constants for hydrogen abstraction reactions of the sulfate radical, SO4−. Alkanes and ethers. Int. J. Chem. Kinet. 21, 611–619. https://doi.org/10.1002/kin.550210802.

Javed, H., Metz, J., Eraslan, T.C., Mathieu, J., Wang, B., Wu, G., Tsai, A.L., Wong, M.S., Alvarez, P.J.J., 2020. Discerning the relevance of superoxide in PFOA degradation. Environ. Sci. Technol. Lett. 7, 653–658. https://doi.org/10.1021/acs.estlett.0c00505.

Lin, H., Niu, J., Xu, J., Li, Y., Pan, Y., 2013. Electrochemical mineralization of sulfamethoxazole by Ti/SnO 2-Sb/Ce-PbO2 anode: kinetics, reaction pathways, and energy cost evolution. Electrochim. Acta 97, 167–174. https://doi.org/10.1016/j.electacta.2013.03.019.

Liu, Fan, X., Quan, X., Fan, Y., Chen, S., Zhao, X., 2019a. Enhanced perfluorooctanoic acid degradation by electrochemical activation of sulfate solution on B/N codoped diamond. Environ. Sci. Technol. 53, 5195–5201. https://doi.org/10.1021/acs.est.8b06130.

Liu, Zhou H., Teng, J., You, S., 2019b. Electrochemical degradation of perfluorooctanoic acid by macro-porous titanium suboxide anode in the presence of sulfate. Chem. Eng. J. 371, 7–14. https://doi.org/10.1016/j.cej.2019.03.249.

Ma, Q., Liu, L., Cui, W., Li, R., Song, T., Cui, Z., 2015. Electrochemical degradation of perfluorooctanoic acid (PFOA) by Yb-doped Ti/SnO2-Sb/PbO2 anodes and determination of the optimal conditions. RSC Adv. 5, 84856–84864. https://doi.org/10.1039/c5ra14299g.

McBeath, S., Wilkinson, D., Graham, N., 2019. Application of boron-doped diamond electrodes for the anodic oxidation of pesticide micropollutants in a water treatment process: a critical review. Environ. Sci. Water Res. Technol. 5, 2090–2107. https://doi.org/10.1039/C9EW00589G.

McBeath, S.T., Graham, N.J.D., 2021. Simultaneous electrochemical oxidation and ferrate generation for the treatment of atrazine: a novel process for water treatment applications. J. Hazard Mater. 411, 125167 https://doi.org/10.1016/j.jhazmat.2021.125167.

McBeath, S.T., Serrano Mora, A., Asadi Zeidabadi, F., Mayer, B.K., McNamara, P., Mohseni, M., Hoffmann, M.R., Graham, N.J.D., 2021. Progress and prospect of anodic oxidation for the remediation of perfluoroalkyl and polyfluoroalkyl substances in water and wastewater using diamond electrodes. Curr. Opin. Electrochem. 30, 100865 https://doi.org/10.1016/j.coelec.2021.100865.

Nzeribe, B.N., Crimi, M., Thagard, S.M., Holsen, T.M., 2019. Physico-chemical processes for the treatment of per-and polyfluoroalkyl substances (PFAS): a review. Crit. Rev. Environ. Sci. Technol. 49, 866–915. https://doi.org/10.1080/10643389.2018.1542916.

Ochiai, T., Iizuka, Y., Nakata, K., Murakami, T., Tryk, D.A., Fujishima, A., Koide, Y., Morito, Y., 2011. Efficient electrochemical decomposition of perfluorocarboxylic acids by the use of a boron-doped diamond electrode. Diam. Relat. Mater. 20, 64–67. https://doi.org/10.1016/j.diamond.2010.12.008.

Olvera-Vargas, H., Wang, Z., Xu, J., Lefebvre, O., 2022. Synergistic degradation of GenX (hexafluoropropylene oxide dimer acid) by pairing graphene-coated Ni-foam and boron doped diamond electrodes. Chem. Eng. J. 430, 132686 https://doi.org/10.1016/j.cej.2021.132686.

Qian, Y., Guo, X., Zhang, Y., Peng, Y., Sun, P., Huang, C.H., Niu, J., Zhou, X., Crittenden, J.C., 2016. Perfluorooctanoic acid degradation using UV-persulfate process: modeling of the degradation and chlorate formation. Environ. Sci. Technol. 50, 772–781. https://doi.org/10.1021/acs.est.5b03715.

Radjenovic, J., Duinslaeger, N., Avval, S.S., Chaplin, B.P., 2020. Facing the challenge of poly- and perfluoroalkyl substances in water: is electrochemical oxidation the answer? Environ. Sci. Technol. 54, 14815–14829. https://doi.org/10.1021/acs.est.0c06212.

Schaefer, C., Andaya, C., Burant, A., Condee, C., 2017. Electrochemical treatment of perfluorooctanoic acid and perfluorooctane sulfonate: insights into mechanisms and application to groundwater treatment. Chem. Eng. J. 317, 424–432.

Sukeesan, S., Boontanon, N., Boontanon, S.K., 2021. Improved electrical driving current of electrochemical treatment of Per- and Polyfluoroalkyl Substances (PFAS) in water using Boron-Doped Diamond anode. Environ. Technol. Innovat. 23, 101655 https://doi.org/10.1016/j.eti.2021.101655.

Trojanowicz, M., Bojanowska-Czajka, A., Bartosiewicz, I., Kulisa, K., 2018. Advanced oxidation/reduction processes treatment for aqueous perfluorooctanoate (PFOA)

and perfluorooctanesulfonate (PFOS) – a review of recent advances. Chem. Eng. J. 336, 170–199. https://doi.org/10.1016/j.cej.2017.10.153.

Urtiaga, A., Fernández-González, C., Gómez-Lavín, S., Ortiz, I., 2015. Kinetics of the electrochemical mineralization of perfluorooctanoic acid on ultrananocrystalline boron doped conductive diamond electrodes. Chemosphere 129, 20–26. https://doi.org/10.1016/j.chemosphere.2014.05.090.

US EPA, 2022. Drinking Water Health Advisories for PFAS, Fact Sheet for Public Water Systems.

Uwayezu, J.N., Carabante, I., Lejon, T., van Hees, P., Karlsson, P., Hollman, P., Kumpiene, J., 2021. Electrochemical degradation of per- and poly-fluoroalkyl substances using boron-doped diamond electrodes. J. Environ. Manag. 290, 112573 https://doi.org/10.1016/j.jenvman.2021.112573.

Vakili, M., Bao, Y., Gholami, F., Gholami, Z., Deng, S., 2021. Removal of HFPO-DA (GenX) from aqueous solutions: a mini-review. Chem. Eng. J. 424, 130266 https://doi.org/10.1016/j.cej.2021.130266.

Van Buren, J., Cuthbertson, A.A., Ocasio, D., Sedlak, D.L., 2021. Ubiquitous production of organosulfates during treatment of organic contaminants with sulfate radicals. Environ. Sci. Technol. Lett. 8, 574–580. https://doi.org/10.1021/acs.estlett.1c00316.

Walsh, F., 1993. Electrochemical Consultancy. In: A First Course in Electrochemical Engineering (Romsey).

Wang, Y., Chang, W., Wang, L., Zhang, Y., Zhang, Y., 2019. A review of sources, multimedia distribution and health risks of novel fluorinated alternatives. Ecotoxicol. Environ. Saf. 182, 109402 https://doi.org/10.1016/j.ecoenv.2019.109402.

Wang, Z., Cousins, I.T., Scheringer, M., Hungerbühler, K., 2013. Fluorinated alternatives to long-chain perfluoroalkyl carboxylic acids (PFCAs), perfluoroalkane sulfonic acids (PFSAs) and their potential precursors. Environ. Int. 60, 242–248. https://doi.org/10.1016/j.envint.2013.08.021.

Yang, S., Fernando, S., Holsen, T.M., Yang, Y., 2019. Inhibition of perchlorate formation during the electrochemical oxidation of perfluoroalkyl acid in groundwater. Environ. Sci. Technol. Lett. 6, 775–780. https://doi.org/10.1021/acs.estlett.9b00653.

Zhuo, Q., Deng, S., Yang, B., Huang, J., Wang, B., Zhang, T., Yu, G., 2012. Degradation of perfluorinated compounds on a boron-doped diamond electrode. Electrochim. Acta 77, 17–22. https://doi.org/10.1016/j.electacta.2012.04.145.

Zhuo, Q., Han, J., Niu, J., Zhang, J., 2020a. Degradation of a persistent organic pollutant perfluorooctane sulphonate with Ti/SnO2–Sb2O5/PbO2-PTFE anode. Emerg. Contam. 6, 44–52. https://doi.org/10.1016/j.emcon.2019.11.002.

Zhuo, Q., Luo, M., Guo, Q., Yu, G., Deng, S., Xu, Z., Yang, B., Liang, X., 2016. Electrochemical oxidation of environmentally persistent perfluorooctane sulfonate by a novel lead dioxide anode. Electrochim. Acta 213, 358–367. https://doi.org/10.1016/j.electacta.2016.07.005.

Zhuo, Q., Wang, J., Niu, J., Yang, B., Yang, Y., 2020b. Electrochemical oxidation of perfluorooctane sulfonate (PFOS) substitute by modified boron doped diamond (BDD) anodes. Chem. Eng. J. 379, 122280 https://doi.org/10.1016/j.cej.2019.122280.